

Demonstration of Directional Modulation Using a Phased Array

Michael P. Daly, *Graduate Student Member, IEEE*, Erica Lynn Daly, and Jennifer T. Bernhard, *Fellow, IEEE*

Abstract—A four-symbol modulation is created by repeated switching of phase shifters in a phased array, in a technique known as directional modulation (DM). The phase shifts are chosen to minimize the bit error rate (BER) in a line-of-sight channel in a desired direction while maximizing the BER elsewhere. A DM transmitter is demonstrated in an anechoic chamber, and results are compared with a traditional baseband QPSK modulation using the same phased array. Experiments indicate that the DM transmitter creates a narrower region of low BERs around the desired direction than the traditional phased array while maintaining high BERs in the sidelobe regions.

Index Terms—Directional modulation, Phase-shift Keying (PSK), phased array, secure communication.

I. INTRODUCTION

THE traditional method of sending digital information using a phased array involves synthesizing the digital signal at baseband and then upconverting to the carrier frequency before sending the signal through the RF portion of the transmitter. Phase shifters are used to synthesize a radiation pattern that meets certain criteria, such as maximizing the power radiated in the desired direction and minimizing it elsewhere. One drawback of this method is that the same information is transmitted in the sidelobes, and that information can still be recovered with a sufficiently sensitive receiver. On the other hand, directional modulation (DM), also called near-field direct antenna modulation (NFDAM), synthesizes the modulation in the RF portion of the transmitter rather than baseband, causing the transmitted digital signal to be direction-dependent [1]–[6].

With DM, the synthesis of a digital modulation can be implemented via parasitic elements of an antenna array [1], [2], [5], phase shifters [4], or driven reconfigurable array elements [3], [6]. DM allows more control over the transmitted modulation, including the ability to send multiple independent signals in different directions with the same RF chain and the ability to scramble a constellation in undesired transmit directions. The distortion of constellations via DM and its security benefits are explained in [4], but until now DM has not been demonstrated with real-time transmission of data. The present work demonstrates a working DM transmitter using a phased array and compares its performance with a transmitter using the same array but

with traditional baseband modulation. Section II provides detail on the implementation of each transmitter and the common receiver. Section III shows the measured performance of both transmitters in the presence of noise and discusses some design tradeoffs.

II. EXPERIMENTAL SETUP

To compare the performance of DM versus baseband modulation, three experiments are conducted for each transmitter where a desired receiver is located in a line-of-sight channel at broadside, -30° , and $+20^\circ$, relative to the transmit array. Eavesdropping receivers may be located in any other direction besides that of the desired receiver, and their locations are not known to the transmitter. A four-element microstrip patch array is used for both transmitters. The array elements are spaced one-half wavelength apart at their operating frequency, 7 GHz. The receive antenna is a standard gain horn oriented to receive the dominant polarization of the microstrip patch array. Signals transmitted in the cross-polarization are not considered in the analysis of the desired receiver or any eavesdropping receiver, and are a subject for future work.

A. Traditional Baseband Array Setup

The experimental procedure of the traditional phased array transmitter will be explained first. A block diagram of the entire arrangement is shown in Fig. 1. The first step for the traditional phased array is to calculate the necessary phase shifts to steer toward the three receiver directions. The calculated phase shifts are stored in a computer located inside an anechoic chamber along with the transmit and receive antennas, and four five-bit Miteq digital phase shifters [7]. The phase shifters are actually six-bit but the number of analog outputs from the computer limits the amount of control bits to five. The phase shifts were calculated assuming isotropic element patterns. Thus, some beamforming error is introduced because the microstrip patch patterns are not entirely constant over the angles of interest, while other error is due to the quantization of the phase shifts. Still, the measured patterns when phased to the three desired directions all have mainlobes of approximately the same magnitude, shown in Fig. 2. Since the mainlobes steered off of broadside are not significantly lower than the mainlobe when all phase shifters are set to 0° , this suggests that the phasing is close to ideal. One other source of error is the presence of a computer inside the anechoic chamber, which slightly distorts the patterns, causing one of the sidelobes in the broadside pattern in Fig. 2 to be about 5 dB higher than the other.

The baseband digital modulation is generated by an Agilent E4438C vector signal generator. A pseudorandom binary sequence (PN15) is sent by the traditional and DM transmitters

Manuscript received August 28, 2009; revised November 06, 2009; accepted November 30, 2009. First published March 01, 2010; current version published May 05, 2010. The work of both M. P. Daly and E. L. Daly was supported by NDSEG Fellowships.

The authors are with the Electromagnetics Laboratory, Department of Electrical and Computer Engineering, University of Illinois at Urbana-Champaign, Urbana, IL 61801 USA (e-mail: mpdaly@illinois.edu; edaly@illinois.edu; jbernhard@illinois.edu).

Digital Object Identifier 10.1109/TAP.2010.2044357

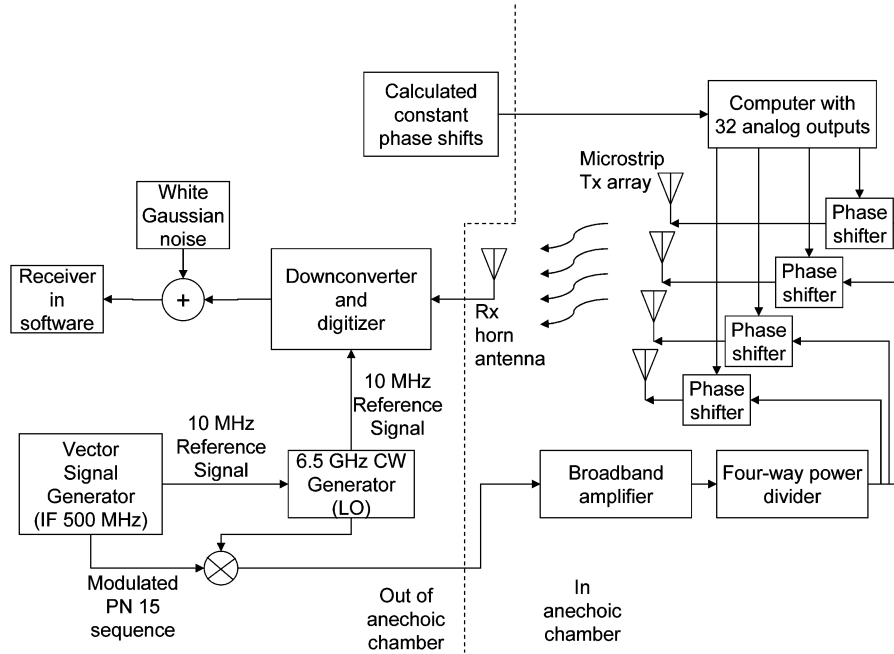


Fig. 1. Experimental configuration of the directional modulation transmitter and receiver.

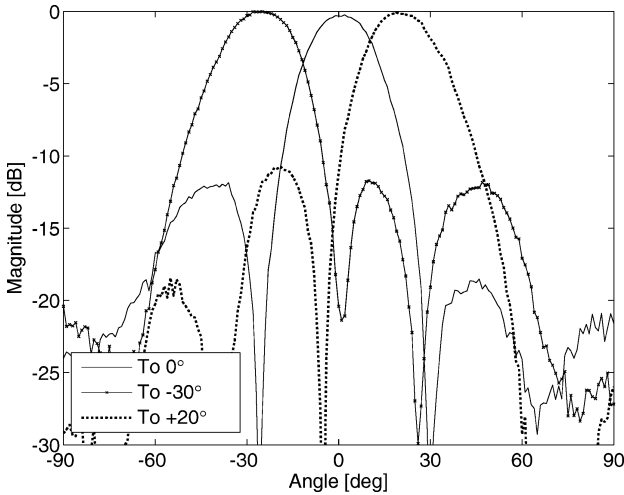


Fig. 2. Normalized measured patterns when the transmit array is steered to broadside, -30° from broadside, and $+20^\circ$ from broadside.

[8]. These information bits are used to create Gray-coded QPSK modulation with a bit rate of 200 kbps that is passed through a root-raised-cosine filter. The vector signal generator upconverts the modulation to an intermediate frequency (IF) of 500 MHz, and it is then externally mixed to 7 GHz. The RF signal is amplified by a broadband amplifier with 21 dB gain and then passes through a four-way power divider before passing through the phase shifters and finally, the antenna array.

After reception by a standard gain horn, root-raised-cosine bandpass filtering, downconversion to baseband, and digital sampling is accomplished by an Agilent E4440A spectrum analyzer. Noise is added to achieve a desired SNR and the signal is demodulated in Matlab [9]. A 10 MHz reference signal between the local oscillator (LO) and the spectrum analyzer makes a phase lock loop (PLL) unnecessary.

B. Directional Modulation Array Setup

The arrangement of the DM transmitter, shown in Fig. 3, differs from the traditional RF transmitter because the modulation is now synthesized in the RF portion. The signal sent into the phase shifters is a sinusoid at the array operating frequency. The signal leaving the phase shifters is modulated due to the fast, repeated changes of the phase shifters, and these modulated signals are not simply delayed copies of each other. Rather, the signals leaving the phase shifters are modulated in a way so that they combine in the far-field to create the desired 4-ary modulation only in the desired direction [4].

Instead of calculating a single set of phase shifts, a set is calculated for each digital symbol (in this case, four). This requires knowledge of the active element patterns, which are measured beforehand. A genetic algorithm (GA) (explained in [4]) calculates the four sets of phase shifts based on the active element patterns with the goal of minimizing the following ratio:

$$\text{Cost} = \frac{\text{BER}(\text{desired direction})}{\min(\text{BER}(\text{undesired directions}))}. \quad (1)$$

In other words, the goal of the GA is to minimize the BER toward the desired receiver while maximizing it elsewhere. There is a “don’t care” region of 5° on either side of the desired direction that is not part of the “undesired directions” in (1) because it is a transition region from low to high BERs. The solutions from the GA are also restricted to those that are possible to be produced by the quantized five-bit phase shifters. In order to increase accuracy, the actual phase shifts of the phase shifters were measured and used in the GA. For example, switching the most significant bit in one of the phase shifters produces a 175.3° shift instead of 180° . As a final step in the GA, the sets of phase shifts were assigned to the four symbols based on Gray coding. Table I shows the set of phase shifts used for communication toward broadside.

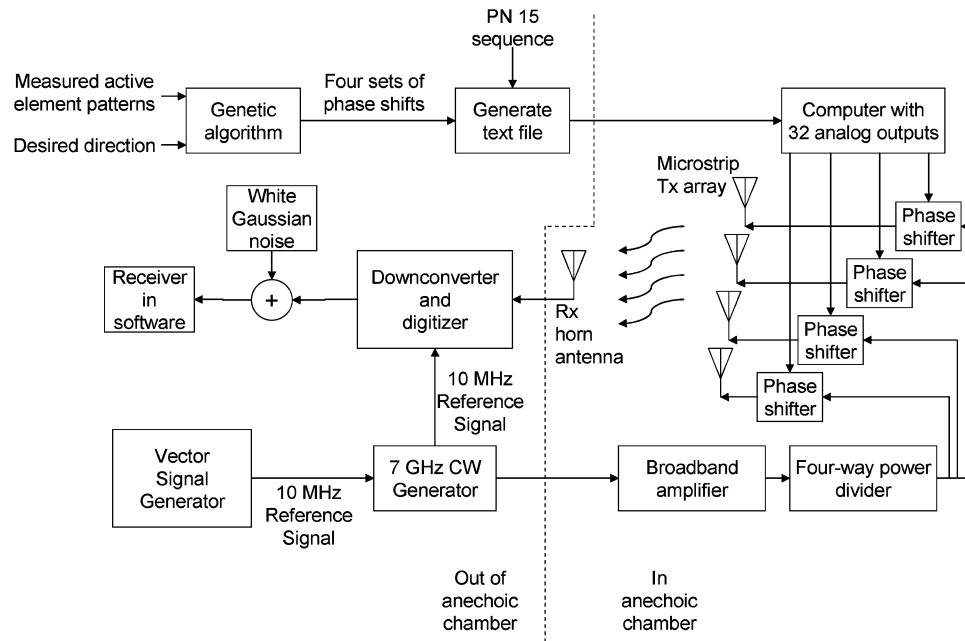


Fig. 3. Experimental configuration of the traditional phased array transmitter and receiver.

TABLE I
SET OF PHASE SHIFTS FOR DM TO PRODUCE FOUR SYMBOLS WHEN THE
DESIRED RECEIVER IS AT BROADSIDE FROM THE TRANSMIT ARRAY

Symbol	Elem. 1	Elem. 2	Elem. 3	Elem. 4
"00"	-143°	-146°	-145°	86°
"01"	-79°	-91°	-74°	-77°
"10"	96°	94°	121°	102°
"11"	42°	-44°	-44°	78°

After the phase shifts are calculated, they are used to construct a text file that governs the real-time switching of the phase shifters. For each symbol consisting of two bits of the pseudo-random binary sequence, control voltages are recorded to produce the corresponding phase shifts for that symbol. Two periods of the binary sequence (32767 symbols) are loaded into a computer containing analog control voltages for the five bits of each phase shifter. The computer repeatedly reads through the entire sequence changing the phase shift control bits at a rate of 100 k Symbols/sec, yielding a bit rate of 200 kbps.

The receiver for DM is nearly the same as the receiver for traditional QPSK modulation. A normal bandpass filter is used instead of a root-raised-cosine filter, since no pulse shaping is done on transmit. The transmitted CW signal still shares a common reference with the downconverter in the receiver, so a phase lock loop is not needed. However, the symbol timing in the DM transmitter is now regulated by the computer controlling the phase shifters, which does not share a common reference with the receiver's sampling clock. Therefore, the received signal is oversampled by a factor of four above the symbol rate and a delay lock loop is implemented to determine the best sampling points.

The bit rate is limited by the speed of the computer producing the analog outputs, since it must produce outputs for 20 control bits each time two bits are transmitted. The switching speed of the phase shifters is actually much faster, on the order

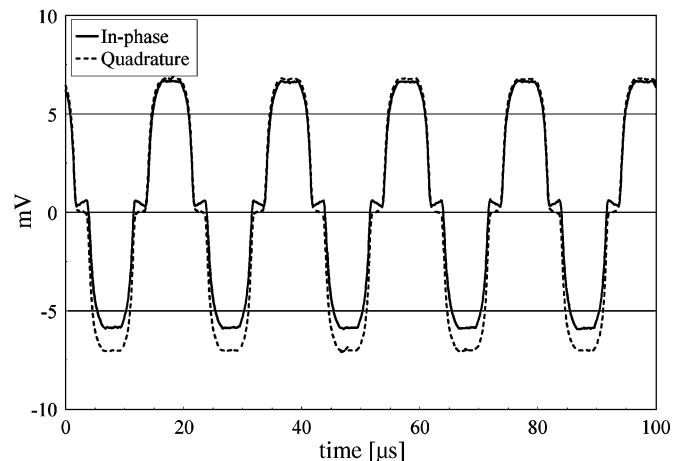


Fig. 4. Measured downconverted output of a phase shifter fed with a 7 GHz CW signal and switched between 0° to 180° at a rate of 100 kHz.

of nanoseconds [7]. The transient effects of switching a phase shifter are shown in Fig. 4. Here, a single phase shifter is connected between a signal generator operating at 7 GHz and the receiver by a wire. The most significant bit (0° to 180°) is repeatedly changed at a rate of 100 kHz. The receiver then downconverts the signal and creates complex baseband samples. Ten periods of switching ($100 \mu\text{s}$) are shown in Fig. 4. It takes about half of the symbol period for the phase shifter to transition, and therefore oversampling by a factor of four guarantees that at least one sample should occur when the transmitted symbol has reached steady state. The discontinuous parts of the curves are likely due to a disallowed bias voltage. When the bias voltage transitions between 0 V and -5 V, there is a point around -2.5 V where both the 0° and 180° modes in the phase shifter are off. This point in the middle of the two bias voltages is what we call the disallowed bias voltage. At this point, the phase shifter's insertion loss increases by about 20 dB, suppressing the signal.

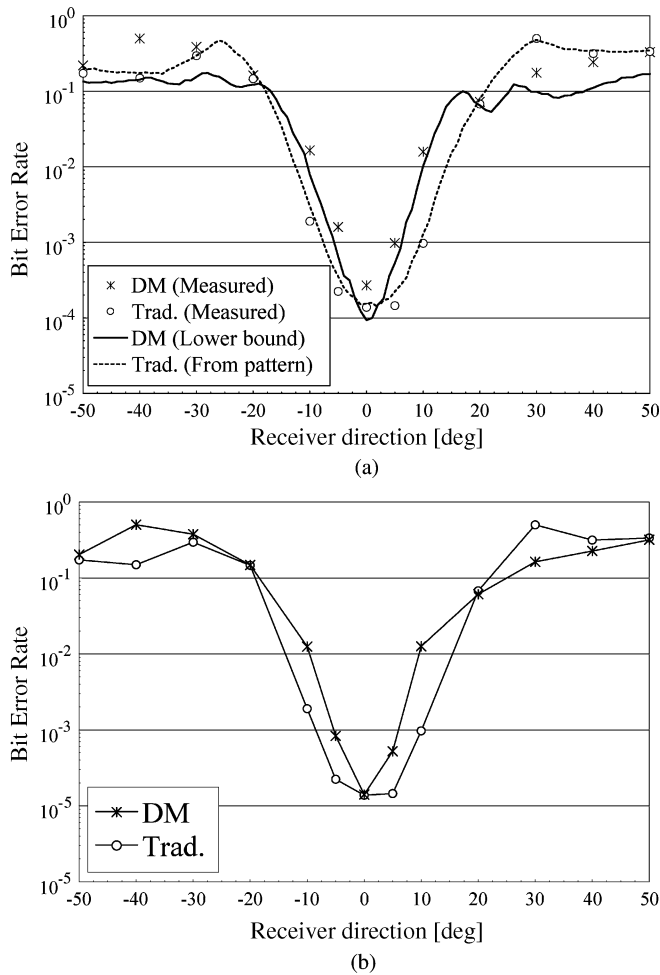


Fig. 5. (a) Measured BERs when both transmitters are directed to broadside. Also shown is the predicted BER of the traditional transmitter based on the measured radiation pattern and the predicted lower bound of the BER of DM based on the measured active element patterns. (b) The noise power in the DM case is decreased by 0.6 dB so that both transmitters achieve the same BER toward the desired receiver at broadside.

III. EXPERIMENTAL RESULTS

In the anechoic chamber, the antenna array for both transmitters was rotated from -50° to $+50^\circ$ while the receiver horn antenna was stationary, to simulate receivers at these directions. Between 1.9 and 2.0 million bits were sent at each direction in 10° increments and white Gaussian noise was added with a noise power of -52 dBm over the frequencies of interest to achieve an SNR of 12 dB in the desired direction. In comparison, the received signals have received power less than -40 dBm. The input power for both transmitters was -7.5 dBm.

Fig. 5(a) shows the BERs of a desired receiver at broadside and other eavesdropping receivers from -50° to $+50^\circ$. Also shown are predicted BER curves based on measured radiation patterns. The predicted BER for the DM transmitter is a lower bound calculated from the GA using the active element patterns [4]. The predicted BER for the traditional transmitter is calculated using the measured pattern data from Fig. 2. The relation between the radiation pattern power and BER for QPSK is given in [4]. The predicted BER for the traditional transmitter agrees well with the measured BER, and the measured BER of

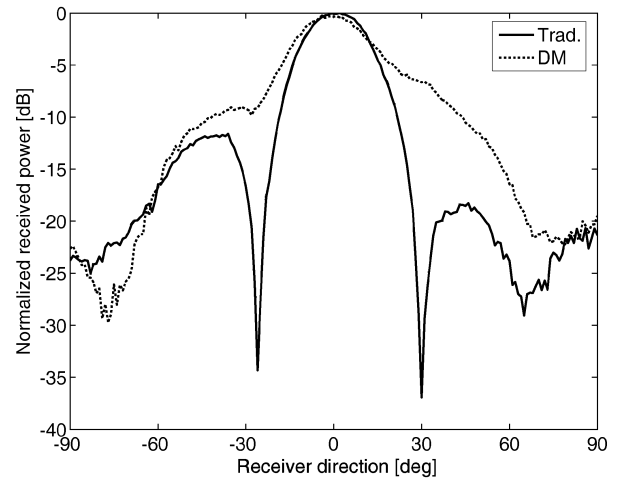


Fig. 6. Average received symbol power by both transmitters when directed toward broadside.

the DM transmitter is always slightly above its calculated lower bound. The close agreement between BERs estimated from radiation patterns and the BERs measured from transmitting a digital modulation is important because it means performance can be accurately assessed when designing a DM transmitter (for example, using the GA in [4], given measured or simulated radiation patterns).

One important feature in Fig. 5(a) is that the BER of the traditional transmitter in the desired direction is less than the BER of the DM transmitter. This is to be expected since the phased array maximizes the power in the broadside direction as its sole priority. On the other hand, the DM transmitter trades some of the power transmitted in the desired direction for a narrower region of low BERs and high BERs in all other directions. This is also evident in Fig. 5(a) in the 20° region around broadside where the BER of an eavesdropper is sometimes an order of magnitude lower if the traditional array is transmitting compared to the DM array.

However, in order to fairly compare the narrowness of the BER regions, the BER in the direction of the desired receiver should be equal for both the DM and traditional transmitters. In the case of the desired receiver at broadside, this is accomplished by raising the signal to noise ratio (SNR) of the DM transmitter 0.6 dB (by lowering the added noise power after signal reception), which lowers the BER in all directions. This new BER curve is shown in Fig. 5(b) along with the same measured BERs of the traditional array from Fig. 5(a). The DM transmitter is able to transmit a low BER in a narrower region than the traditional transmitter, confirming the results first calculated in [4].

The reason the DM transmitter produces a narrower low BER region can be found from the received power and the received constellations. Fig. 6 shows the average received symbol power calculated from the radiation pattern of the traditional transmitter and the active element patterns of the DM transmitter. This received symbol power was used to calculate the predicted BER curves in Fig. 5(a). Since all constellation points have the same magnitude in the traditional array with QPSK, the average symbol power equals the instantaneous symbol power. On the

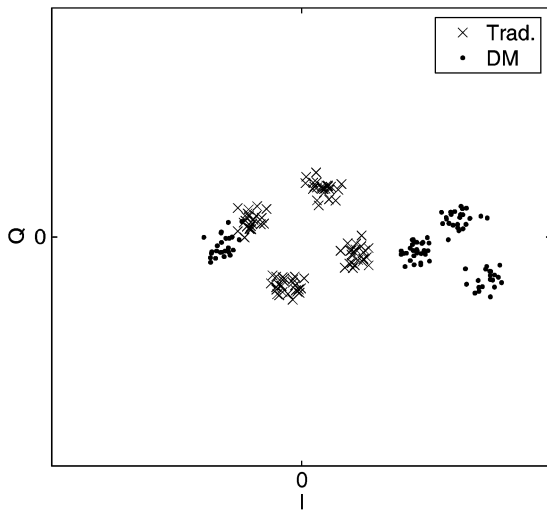


Fig. 7. Received constellations from both transmitters by an eavesdropping receiver at $+50^\circ$ when both transmitters directed toward broadside.

other hand, the DM array creates arbitrary constellations with different power for different symbols, so average symbol power is used to compare the two methods.

Toward the desired receiver at broadside, the two transmitters send about the same power (after increasing the DM transmitter power by 0.6 dB). But off broadside, the DM array tends to send more power than the traditional array. Yet, the measured BERs are either lower for the DM array or about the same as the traditional array. The reason for this can be gleaned from the received constellation. For example, the first 200 received constellation points that would be seen by an eavesdropper at $+50^\circ$ when the DM and traditional transmitters are intending to transmit to 0° is shown in Fig. 7. From Fig. 6, the symbol power calculated from radiation patterns is 7.7 dB higher at $+50^\circ$ for the DM array than the traditional array. When actually measured by sending digital signals, the received power was 7.6 dB higher for the DM array than the traditional array. The BER measured at $+50^\circ$ was approximately the same for both transmitters (0.20 for the traditional array and 0.16 for the DM array). The reason the DM array achieves this same high BER toward the eavesdropper while transmitting at a higher power level is evident from the constellation diagram. Three of the constellation points are grouped close together, even though they are far from the origin. This indicates three signals with higher power that look approximately the same, and thus are difficult to demodulate correctly. The traditional baseband constellations are the same shape regardless of where the receiver is located, so the only way to increase BER and reduce the chance of demodulation by an eavesdropper is to reduce the power of each symbol, or equivalently reduce the sidelobe level in the radiation pattern.

Figs. 8 and 9(a) show the predicted and measured BER when the desired receiver is at -30° and $+20^\circ$, respectively. These figures have the same characteristics as Fig. 5(a). The low BER region is narrower for the DM transmitter than the traditional transmitter, while the BERs are approximately equal between the two transmitters in the sidelobe region. In the case when the desired receiver is at -30° , both transmitters produce the same BER at -30° with equal input power, due to the fact that the

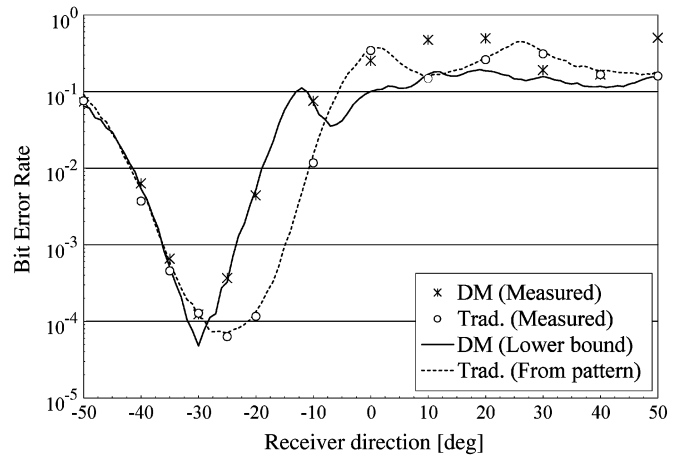
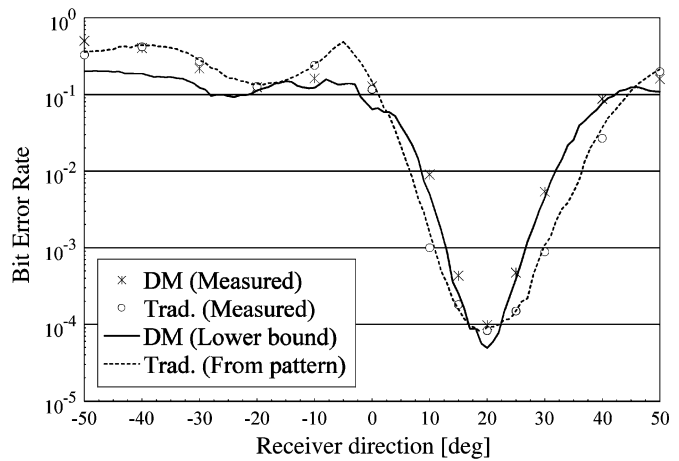
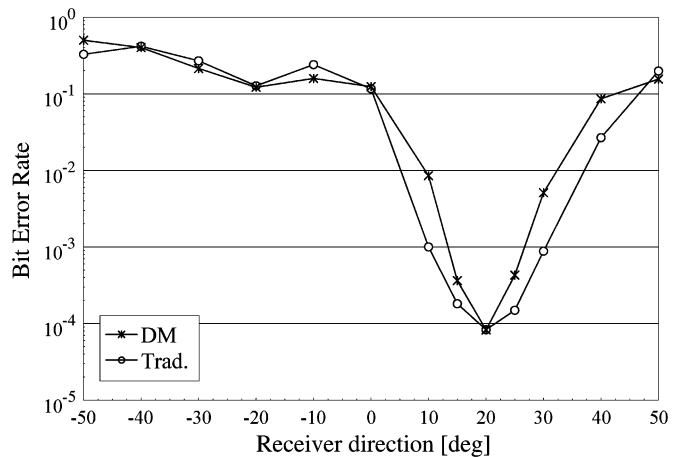


Fig. 8. Measured BERs when both transmitters are directed to -30° . Also shown is the predicted BER of the traditional transmitter based on the measured radiation pattern and the predicted lower bound of the BER of DM based on the measured active element patterns.



(a)



(b)

Fig. 9. (a) Measured BERs when both transmitters are directed to $+20^\circ$. Also shown is the predicted BER of the traditional transmitter based on the measured radiation pattern and the predicted lower bound of the BER of DM based on the measured active element patterns. (b) The noise power in the DM case is decreased by 0.1 dB so that both transmitters achieve the same BER toward the desired receiver at broadside.

traditional array's maximum of the radiation pattern occurs at -26° rather than -30° .

In the case when the desired receiver is at $+20^\circ$ from array broadside, the DM transmitter produced the same BER as the traditional transmitter toward $+20^\circ$ when the SNR of the DM transmitter was increased by 0.1 dB, shown in Fig. 9(b). The region of low BER once again is narrower for the DM transmitter.

IV. CONCLUSION

This work presents the first experimental demonstration of directional modulation by transmitting data in real-time. The results agree well with the calculated results from [4], indicating that a DM transmitter manipulates a direction-dependent signal so that it is harder to decode in more undesired directions. In addition, the DM array sends a signal that will be decoded by the desired receiver with the same low BER (with some small increase in transmit power possibly necessary) with no additional work needed by the receiver.

Future work consists of other implementations of DM, including using vector modulators so that both magnitude and phase of each antenna element can be manipulated. Another area of research is the real-time demonstration of DM using reconfigurable radiating elements. The synthesis of more complex modulations, the use of radiated cross-polarized fields, and incorporation into non-line-of-sight channels are also being explored.

REFERENCES

- [1] A. Babakhani, D. B. Rutledge, and A. Hajimiri, "A near-field modulation technique using antenna reflector switching," in *Proc. IEEE Int. Solid State Circuits Conf.*, Feb. 2008, pp. 188–189.
- [2] A. Babakhani, D. B. Rutledge, and A. Hajimiri, "Transmitter architectures based on near-field direct antenna modulation," *IEEE J. Solid State Circuits*, vol. 43, no. 12, pp. 2674–2692, Dec. 2008.
- [3] M. P. Daly and J. T. Bernhard, "Reconfigurable array for multi-directional and secure communication," in *Proc. Allerton Antennas Symp.*, Monticello, IL, Sep. 2008, pp. 116–131.
- [4] M. P. Daly and J. T. Bernhard, "Directional modulation technique for phased arrays," *IEEE Trans. Antennas Propag.*, vol. 57, pp. 2633–2640, Sep. 2009.
- [5] A. Chang, A. Babakhani, and A. Hajimiri, "Near-field direct antenna modulation (NFDAM) transmitter at 2.4 GHz," in *Proc. IEEE Antennas Propag. Soc. Int. Symp.*, Jun. 2009, pp. 1–4.
- [6] M. P. Daly and J. T. Bernhard, "Beamsteering in pattern reconfigurable arrays using directional modulation," *IEEE Trans. Antennas Propag.*, accepted for publication.
- [7] Digital Phase Shifters, MITEQ, Inc. [Online]. Available: <http://amps.miteq.com/datasheets/MITEQ-DPS.PDF>
- [8] B. P. Lathi, *Modern Digital and Analog Communication Systems*, 3rd ed. New York: Oxford Univ. Press, 1998.
- [9] MATLAB Version 7.0.4.365 (R14) Service Pack 2, The Mathworks, Inc., Natick, MA, 2005.



Michael P. Daly (S'09) was born in San Juan, Puerto Rico, on October 31, 1984. He received the B.S. degree (with highest honors) and M.S. degree in electrical engineering at the University of Illinois at Urbana-Champaign (UIUC), in 2007 and 2008, respectively, where he is currently working toward the Ph.D. degree.

His research interests include reconfigurable antennas, arrays, and digital communications.

Mr. Daly is the recipient of an NDSEG fellowship.



Erica Lynn Daly was born in 1985 in Chicago, IL. Since 2003, she has studied electrical engineering at the University of Illinois at Urbana-Champaign, where she is currently working toward the Ph.D. degree.

Her research interests include signal processing and applied communication theory.

Mrs. Daly is the recipient of an NDSEG fellowship.



Jennifer T. Bernhard (S'89–M'95–SM'01–F'10) was born on May 1, 1966, in New Hartford, NY. She received the B.S.E.E. degree from Cornell University in 1988 and the M.S. and Ph.D. degrees in electrical engineering from Duke University in 1990 and 1994, respectively, with support from a National Science Foundation Graduate Fellowship.

While at Cornell, she was a McMullen Dean's Scholar and participated in the Engineering Co-op Program, working at IBM Federal Systems Division in Owego, New York. During the 1994–95 academic

year she held the position of Postdoctoral Research Associate with the Departments of Radiation Oncology and Electrical Engineering at Duke University, where she developed RF and microwave circuitry for simultaneous hyperthermia (treatment of cancer with microwaves) and MRI (magnetic resonance imaging) thermometry. At Duke, she was also an organizing member of the Women in Science and Engineering (WISE) Project, a graduate student-run organization designed to improve the climate for graduate women in engineering and the sciences. From 1995–1999, she was an Assistant Professor in the Department of Electrical and Computer Engineering at the University of New Hampshire, where she held the Class of 1944 Professorship. Since 1999, she has been with the Electromagnetics Laboratory in the Department of Electrical and Computer Engineering at University of Illinois at Urbana-Champaign, where she is now a Professor. In 1999 and 2000, she was a NASA-ASEE Summer Faculty Fellow at NASA Glenn Research Center in Cleveland, OH. She was also an Illinois College of Engineering Willett Faculty Scholar and is a Research Professor in Illinois' Micro and Nanotechnology Laboratory, the Coordinated Science Laboratory, and the Information Trust Institute. Her industrial experience includes work as a research engineer with Avnet Development Labs and, more recently, as a private consultant for members of the wireless communication and sensors community. Her research interests include reconfigurable and wideband microwave antennas and circuits, wireless sensors and sensor networks, high speed wireless data communication, electromagnetic compatibility, and electromagnetics for industrial, agricultural, and medical applications, and has two patents on technology in these areas.

Prof. Bernhard received the NSF CAREER Award in 2000. She and her students received the 2004 H. A. Wheeler Applications Prize Paper Award from the IEEE Antenna and Propagation Society for their paper published in the March 2003 issue of the IEEE TRANSACTIONS ON ANTENNAS AND PROPAGATION. She served as an Associate Editor for IEEE TRANSACTIONS ON ANTENNAS AND PROPAGATION from 2001–2007 and served as an Associate Editor for IEEE ANTENNAS AND WIRELESS PROPAGATION LETTERS from 2001–2005. She is also a member of the editorial board of *Smart Structures and Systems*. She is a member of URSI Commissions B and D, Tau Beta Pi, Eta Kappa Nu, Sigma Xi, and ASEE. She is a Fellow of the IEEE and served as an elected member of the IEEE Antennas and Propagation Society's Administrative Committee from 2004–2006. She was President Elect and President of the IEEE Antennas and Propagation Society in 2007 and 2008, respectively.